

Marine reservoir ages for coastal West Africa

Guillaume Soulet¹, Philippe Maestrati², Serge Gofas^{2,3}, Germain Bayon¹, Fabien Dewilde¹, Maylis Labonne⁴, Bernard Dennielou¹, Franck Ferraton⁴, Giuseppe Siani⁵

1 Ifremer, Univ Brest, CNRS, Geo-Ocean UMR6538, F-29280, Plouzané, France

5 2 Muséum National d'Histoire Naturelle, Paris, DGD-Collections, France

3 Departamento de Biología Animal, Facultad de Ciencias, Universidad de Málaga, Málaga, Spain

4 MARBEC, Univ Montpellier, CNRS, Ifremer, IRD, Montpellier, France

5 GEOPS, UMR 8148 Université Paris-Saclay, Orsay, France

Correspondence to: Guillaume Soulet (gsoulet@ifremer.fr)

10 **Abstract.** We measured the ¹⁴C age of pre-bomb suspension-feeding bivalves of known-age from coastal West Africa (~~n=30~~)
across a latitudinal transect extending from 33°N to 15°S. The specimens are from the collections of the Muséum National
d'Histoire Naturelle (Paris, France). They were carefully chosen to ensure that the specimens were alive when collected or
died not long before collection. From the ¹⁴C-dating of these known-age bivalves, we calculated the marine reservoir age (as
ΔR and R values) for each specimen. ΔR values were calculated relative to the Marine20 calibration curve and the R values
15 relative to Intcal20 or SHcal20 calibration curves. Except for five outliers, the ΔR and R values were quite homogenous to a
weighted mean value of $-77-72 \pm 47-42$ ¹⁴C yrs (1sd, n = 2524), and of $400-406 \pm 59-56$ ¹⁴C yrs (1sd, n = 2524), respectively.
These values are typical of low latitude marine reservoir age values. Five suspension-feeding species living in five different
ecological habitats were studied. For localities where different species were available, the results yielded similar results
whatever the species/species considered suggesting that in these locations the habitat has only a limited impact on the marine
20 reservoir age reconstruction. We show that our measured marine reservoir ages follow the declining trend of the global marine
reservoir age starting ca. 1900 AD, suggesting that marine reservoir age of coastal West Africa is driven, at least at first order,
by the global carbon cycle and climatethe atmospheric CO₂ ¹⁴C ageing due to fossil fuel burning rather than by local effects.
Each outlier was discussed. Local upwelling conditions or Subsub-fossil specimens likely may explain the older ¹⁴C age and
thus larger marine reservoir age measured for these samples. *Bucardium ringens* might not a best choice for marine reservoir
25 age reconstructions.

1 Introduction

The marine reservoir age (R) at a given calendar time/year (t) is the difference between the radiocarbon age (¹⁴C) of the
dissolved inorganic carbon (DIC) of the ocean (¹⁴C_m) and that of atmospheric CO₂ (¹⁴C_{atm}) (Stuiver et al., 1986; Stuiver and
Braziunas, 1993)(Stuiver and Polach, 1977; Ascough et al., 2005; Soulet et al., 2016; Skinner and Bard, 2022; Soulet, 2015):

$$30 \quad R(t) = {}^{14}\text{C}_m(t) - {}^{14}\text{C}_{\text{atm}}(t) \quad (1)$$

At global scale, the marine reservoir age of the surface mixed layer of the ocean is set by the exchange of “young” CO₂ at the atmosphere-ocean interface, plus the exchange of DIC between oceanic surface waters and deep waters that contain large amounts of “old” DIC (Bard, 1988; Skinner and Bard, 2022). [Box models have been used to study the distribution of radiocarbon in Earth’s system since the 1950s \(Craig, 1957; Revelle and Suess, 1957; Arnold and Anderson, 1957; Siegenthaler, 1983\).](#) The ¹⁴C age of the global ocean over time, i.e., the Marine20 calibration curve (Heaton et al., 2020), has been modelled using the global carbon cycle box model BICYCLE (Köhler et al., 2006; Köhler and Fischer, 2006, 2004; Köhler et al., 2005) and the Northern Hemisphere atmospheric ¹⁴C calibration curve (IntCal20; Reimer et al., 2020). While the global marine calibration curve (Marine20) is widely used to derive calibrated ages from ¹⁴C dating of marine samples, it does not account for local marine ¹⁴C offsets due to, for instance, continental carbon inputs to the coastal ocean, regional winds, and changes in the oceanic circulation and climate (Bard, 1988; Alves et al., 2018; Skinner and Bard, 2022; Heaton et al., 2023). Hence, the usefulness of the ΔR metric (Stuiver et al., 1986; Stuiver and Braziunas, 1993; Reimer and Reimer, 2017) that is the difference between the ¹⁴C age of any marine sample (¹⁴C_m) and that of the marine calibration curve (¹⁴C_{Marine20}) at the same time (t):

$$\Delta R(t) = {}^{14}\text{C}_m(t) - {}^{14}\text{C}_{\text{Marine20}}(t) \quad (2)$$

The local marine reservoir age offset (ΔR) is known to vary largely as demonstrated by pre-bomb values ranging between – 500 to + 2000 ¹⁴C years (Reimer and Reimer, 2001) depending on the location. [Most Larger-larger](#) ΔR values are located at high-latitudes while values close to ΔR = 0 ¹⁴C years are located at low latitudes (Bard, 1988; Bard et al., 1994).

From a geochronological perspective (i.e., calibration of marine ¹⁴C dates and building age-depth models from marine ¹⁴C dates), knowing ΔR(t) is of crucial interest to correct marine ¹⁴C dates for a local ¹⁴C offset compared to the global marine calibration curve and hence a pre-requirement to derive accurate calendar ages. Reconstructing ΔR(t) values from unstudied areas is also valuable as it could contribute to deriving regional/local marine calibration curves from the global one using 3-D large-scale ocean circulation model (Butzin et al., 2017; Alves et al., 2019).

From a carbon cycle perspective, the R(t) and ΔR(t) are also very important as they reflect ¹⁴C disequilibria between the ocean and the atmosphere and hence they are key proxies to understand local variations of the global carbon cycle, and its evolution over time with changing climate and environment (Skinner et al., 2015, 2010; Lindsay et al., 2016; Soulet et al., 2011; Siani et al., 2001; Schefuß et al., 2016; Heaton et al., 2021).

On a whole, efforts to estimate R(t) and ΔR(t) values wherever possible are valuable to the understanding of both modern and past carbon cycle, and the reconstruction of climate and environmental changes based on sedimentary archives.

Pre-bomb R(t) and ΔR(t) values for coastal West Africa are very sparse. According to the Marine Reservoir Correction Database (Reimer and Reimer, 2001; <http://calib.org/marine/>; last seen 15/11/2022), from Oran on the Mediterranean coast of Algeria (Siani et al., 2000) to Hondelkip Bay on the Atlantic coast of South Africa (Dewar et al., 2012), only [a](#) few marine reservoir ages from Mauritania and Senegal were reported (Ndeye, 2008) (Fig. 1). For Mauritania, collection sites were Nouadhibou (formerly Port-Étienne, 2 samples), the area of the Cape Timiris – El Mamghar (3 samples). Two samples were collected from an unknown location from coastal Mauritania. For Senegal, collection sites were restricted to the Dakar area

65 (Almadies, Dakar harbour, Gorée Island and Rufisque; 5 samples). Thirteen additional samples were from unknown locations from coastal Senegal.

In this study we report new marine reservoir age values (n=30) based on the ^{14}C dating of bivalves with a known pre-bomb collection date and collected across a latitudinal transect extending from Mohammedia (Morocco, 33°N) to Moçâmedes (Angola, 15°S). Our suite of sample includes specimens from Mauritania, Senegal, Republic of Guinea, Sierra Leone, Ivory
70 Coast, Benin, Gabon and Republic of Congo (Fig. 1, Table S1 in the Supplement). We used specimens of five different species: *Senilia senilis*, *Bucardium ringens*, *Donax rugosus*, *Ostrea stentina* and *Pseudochama gryphina*. We briefly discuss our results in the context of local environmental setting of the studied bivalves and regional oceanography of the Eastern Atlantic Ocean.

2 Material and methods

2.1 Material

75 Bivalve shells were selected from the collections of the Muséum National d'Histoire Naturelle (MNHN) (Paris, France). We carefully chose pre-bomb specimens of known-age and ensured that they were collected alive or very soon after death. For example, specimens with articulated valves and exhibiting flesh remains inside the shell were clearly collected alive. For *Senilia senilis*, the presence of the fragile periostracum provides evidence that the specimen was collected fresh. For *Bucardium ringens*, remains of the hinge ligament indicate that the bivalve death occurred not long before collection. The collection date
80 was also carefully checked. Below, we provide background information for the five different bivalve species investigated in this study. Additional information for each sample is given in section 3.1.

Senilia senilis (Linnaeus, 1758) can be found from Mauritania to northern Angola. It lives in fine sand in estuaries, creeks or lagoon with regular tidal influence from the lower intertidal zone to about 2 meters water depth. The [species](#) is tolerant to seasonal salinity changes (von Cosel and Gofas, 2019). *S. senilis* is a suspension feeder that lives in the top 5-10-cm layer
85 of the sediment (Okera, 1976; Catry et al., 2017).

Bucardium ringens (Bruguière, 1789) occurs from Mauritania to southern Angola. It lives in clean fine sand and mixed sand on open coast from shallow (5-10 meters depth) to about 50 meters depth. Shells and valves are commonly cast ashore on beaches but live-taken specimens are rare (von Cosel and Gofas, 2019). *B. ringens* is likely a suspension feeder as typically are cardiids (Herrera et al., 2015).

90 *Donax rugosus* (Linnaeus, 1758) occurs from Mauritania to Ghana and from northern Angola to southern Angola. It lives in mixed and coarse sand in the surf zone of open beaches (von Cosel and Gofas, 2019). *D. rugosus* is a suspension feeder (Smith, 1971).

Ostrea stentina (Payraudeau, 1826) can be found [from](#) southern Portugal to Ghana, then from Gabon to northern Angola. It is common and occurs on various types of hard substrate such as rocks, stones, pebbles and other oysters from 1 to 30 meters
95 depths. It can also be found in lagoons, inlets and creeks under marine condition (von Cosel and Gofas, 2019). *O. stentina* is a suspension feeder (Türkmen et al., 2005).

Pseudochama gryphina (Lamarck, 1819) occurs from Southern Portugal to Mauritania and from Gabon to southern Angola (von Cosel and Gofas, 2019) and lives on hard substrate such as rocks and stones in clear water offshore about 10 to 60 meters water depth. *P. gryphina* is a suspension feeder (Sessa et al., 2013).

100 A small piece (30-100 mg) of the outermost layers of each shell was cut using a Dremel™ rotary tool fitted with a cut-off wheel. We focused on the external part of the shell to ensure that we sampled and dated the most recent part (likely the last few months) of the specimen. The shell carbonate samples were then sonicated and rinsed in deionized water at least 5 times. Samples were coarsely crushed and split into a subsample for stable isotopic analysis and a subsample for ¹⁴C analysis.

2.2 Radiocarbon measurements

105 Samples were washed with dilute HNO₃ (0.01M) for 15 min then rinsed to neutral pH. Then the shell carbonate was converted into CO₂ following LMC14 laboratory (Laboratoire de Mesure du Radiocarbone, Saclay, France) standard phosphoric acid hydrolysis procedure (Tisnérat-Laborde et al., 2001; Dumoulin et al., 2017). The CO₂ was then converted to graphite (Cottéreau et al., 2007; Dumoulin et al., 2017) and analyzed for its ¹⁴C composition by Accelerator Mass Spectrometry (AMS) using the Artémis ¹⁴C AMS facility (Moreau et al., 2013). Results are corrected for the ¹³C/¹²C ratio as measured on the AMS
110 (Santos et al., 2007) and are reported in the F¹⁴C notation (Reimer et al., 2004). F¹⁴C is identical to the A_{SN}/A_{ON} metric (Stuiver and Polach, 1977), and the ¹⁴a_N notation (Mook and van der Plicht, 1999). Corresponding conventional ¹⁴C ages reported in ¹⁴C years Before Present (AD 1950) were calculated according to:

$${}^{14}\text{C} = -8033\ln(\text{F}^{14}\text{C}) \quad (3)$$

2.3 Stable carbon isotopes

115 Stable carbon and oxygen isotopic analyses of the dated samples were performed at the Pôle Spectrométrie Océan (PSO, Plouzané, France) using a MAT-253 (Thermo Scientific) stable isotope ratio mass spectrometer (IRMS) coupled with a Kiel IV Carbonate Device (Thermo Scientific). The measurements are reported versus Vienna Pee Dee Belemnite standard (VPDB) defined with respect to two international carbonate standards: NBS-19 ($\delta^{18}\text{O} = -2.20 \text{ ‰}$ and $\delta^{13}\text{C} = +1.95 \text{ ‰}$) and NBS-18 ($\delta^{18}\text{O} = -23.20 \text{ ‰}$ and $\delta^{13}\text{C} = -5.01 \text{ ‰}$). The mean external reproducibilities (1 σ), based on repeated measurements of
120 an in-house standard, was $\pm 0.04 \text{ ‰}$ and $\pm 0.02 \text{ ‰}$ for $\delta^{18}\text{O}$ and $\delta^{13}\text{C}$ values, respectively. [Note that our samples integrate a seasonal variability of up 0.5 to 1‰ as shown by several investigations of growth layers in shells \(e.g., Carré et al., 2005; Jones et al., 2007, 2010\).](#)

2.4 Marine Reservoir Age calculation

The marine reservoir age R of the selected shells is calculated according to equation (1) where t is the collection year as known
125 from the museum records (Table S1 in the Supplement and section results), ¹⁴C_m is the measured shell ¹⁴C age, and ¹⁴C_{atm} is the ¹⁴C age of the atmosphere. For shells picked from the northern hemisphere, ¹⁴C_{atm} is obtained from the IntCal20 calibration

curve (Reimer et al., 2020). For shells from the southern hemisphere, we used instead the southern hemisphere calibration curve SHCal20 (Hogg et al., 2020). The uncertainty is calculated (Soulet, 2015) according to:

$$\sigma_{R(t)} = \sqrt{\sigma_{^{14}\text{C}_m(t)}^2 + \sigma_{^{14}\text{C}_{\text{atm}}(t)}^2} \quad (4)$$

130 Note that mean SHCal20 offset compared to IntCal20 is estimated to be 36 ± 27 ^{14}C yrs. Thus, the R values calculated with IntCal20 or SHcal20 are essentially the same if one takes uncertainties into account.

The local marine reservoir offset ΔR of the selected shells is calculated according to equation (2) where t is the collection year as known from the museum records (Table S1 in the Supplement and section results), $^{14}\text{C}_m$ is the measured shell ^{14}C age, and $^{14}\text{C}_{\text{Marine20}}$ is the ^{14}C age of the global marine calibration curve. The uncertainty is calculated as follows:

$$135 \quad \sigma_{\Delta R(t)} = \sqrt{\sigma_{^{14}\text{C}_m(t)}^2 + \sigma_{^{14}\text{C}_{\text{Marine20}}(t)}^2} \quad (5)$$

Note that Reimer and Reimer (2017) do not propagate the uncertainty of Marine20 calibration curve.

3 Results and Discussion

3.1 Radiocarbon measurements results

The results are shown in Table S1 in the Supplement. Below we provide the detailed list of the samples used in this study. We classified the samples by location with corresponding geographic coordinates, then by species. Code numbers “MNHN-IM-2022-xxxx” allows one to find the samples in the collections of the MNHN of Paris (France). Code numbers “SacA-xxxxx” are the radiocarbon laboratory number for the sample.

3.1.1 Samples from Morocco

MNHN-IM-2022-4615

145 *Ostrea stentina*

Mohammedia (33.71°N, 7.37°W)

Articulated specimen with remains of flesh.

SacA-68834: 482 ± 18 BP

$F^{14}\text{C} = 0.9418 \pm 0.0021$

150 $\delta^{13}\text{C} = 1.19$ ‰ VPDB

~~Collection date~~Collection date (AD): 1921

Collector: Jacques de Lépiney

Museum label: *Ostrea stentina* Payr, Fedhala 1921, donat J de Lépiney 1939

155 MNHN-IM-2022-4609

Ostrea stentina

El Jadida, beach (33.25°N, 8.49°W)

An isolated valve looking quite fresh.

SacA-68828: 817 ± 18 BP

160 F¹⁴C = 0.9033 ± 0.0020

δ¹³C = 0.71 ‰ VPDB

~~Collection date~~ [Collection date \(AD\)](#): October 26th 1909

Collector: Louis Gentil

Museum label: Plage de Mazagan 26 octobre 1909, Maroc, Louis Gentil

165

MNHN-IM-2022-4608

Ostrea stentina

Lagoon of Sidi Moussa (32.98°N, 8.75°W)

Articulated specimen with remains of flesh.

170 SacA-68827: 1058 ± 19 BP

F¹⁴C = 0.8766 ± 0.0021

δ¹³C = -0.48 ‰ VPDB

~~Collection date~~ [Collection date \(AD\)](#): 1924

Collector: Jacques de Lépiney

175 Museum label: *Ostrea stentina* Payr., lagune de Sidi Moussa (région de Mazagan), 1924, donat. J de Lépiney 1939

3.1.2 Samples from Mauritania

MNHN-IM-2022-4612

Ostrea stentina

Nouadhibou, Pointe Chacal (20.91°N, 17.04°W)

180 Articulated specimen.

SacA-68831: 514 ± 17 BP

F¹⁴C = 0.9381 ± 0.0020

δ¹³C = 2.28 ‰ VPDB

~~Collection date~~ [Collection date \(AD\)](#): 1948

185 Collector: Roger Sourie

Museum label: Port Etienne (Pointe des Chacals) M. Sourie, 1948

MNHN-IM-2022-4610

Ostrea stentina

190 Cansado Bay (20.88°N, 17.04°W)

Articulated specimen with remains of flesh.

SacA-68829: 516 ± 17 BP

F¹⁴C = 0.9378 ± 0.0020

δ¹³C = 2.09 ‰ VPDB

195 ~~Collection date~~ [Collection date \(AD\)](#): 1911-1912

Collector: Mission Gruvel

Museum label: *Ostrea stentina* Payr. = *lacerans* Hanl., Baie de Cansado, Mission Gruvel, 1911-1912

MNHN-IM-2022-4599

200 *Bucardium ringens*

Nouadhibou (20.88°N, 17.04°W)

An isolated valve of a juvenile with remains of the hinge ligament.

SacA-68811: 863 ± 18 BP

F¹⁴C = 0.8981 ± 0.0020

205 δ¹³C = 0.38 ‰ VPDB

~~Collection date~~ [Collection date \(AD\)](#): 1908

Collector: Mission Gruvel

Museum label: *Cardium ringens* Gmelin; Port Etienne; 1908; Mission Gruvel

210 MNHN-IM-2022-4603

Donax rugosus

Ndiago, beach (16.17°N, 16.51°W)

Articulated specimen with remains of flesh and hinge ligament.

SacA-68815: 518 ± 19 BP

215 F¹⁴C = 0.9376 ± 0.0022

δ¹³C = 0.68 ‰ VPDB

~~Collection date~~ [Collection date \(AD\)](#): January 21st 1908

Collector: Mission Gruvel

Museum label: *Donax rugosus* Linné, N'Diago plage, 21.I.08, Mission Gruvel

220 **3.1.3 Samples from Senegal**

MNHN-IM-2022-4607

Donax rugosus

Saint Louis (16.02°N, 16.51°W)

Articulated specimen with remains of flesh and hinge ligament.

225 SacA-68819: 574 ± 18 BP

F¹⁴C = 0.9310 ± 0.0021

δ¹³C = 1.29 ‰ VPDB

~~Collection date~~ [Collection date \(AD\)](#): December 1901

Collector: Buchet's mission

230 Museum label: Sénégal, Saint Louis, Coquilles; Donax, M^{on} Buchet, X^{bre} 1901

MNHN-IM-2022-4592

Senilia senilis

Dakar, backwaters of the "Marigot de Hann" (14.74°N, 17.39°W)

235 Articulated specimen with remains of flesh and well-preserved periostracum.

SacA-68824: 560 ± 17 BP

F¹⁴C = 0.9327 ± 0.0020

δ¹³C = -0.29 ‰ VPDB

~~Collection date~~ [Collection date \(AD\)](#): May 1908

240 Collector: Mission Gruvel

Museum label: Arca (*Senilia*) *senilis* Linné, Marigot de Hann V.1908, se vend sur le marché de Dakar env. 2 sous la douzaine, Mission Gruvel

Note: The Marigot of Hann seems to have been a creek more or less connected to the ocean. It was drawn on a map of Dakar in 1905 but does not exist any longer. The map can be accessed from the Gallica website managed by the Bibliothèque

245 Nationale de France: <https://gallica.bnf.fr/ark:/12148/btv1b53197802m>

MNHN-IM-2022-4593

Senilia senilis

Dakar, Bay of Hann, Pointe Bel Air, beach at low tide (14.71°N, 17.42°W)

250 Articulated specimen with remains of flesh and well-preserved periostracum.

SacA-68825: 544 ± 18 BP

F¹⁴C = 0.9346 ± 0.0020

$\delta^{13}\text{C} = 0.07 \text{‰ VPDB}$

[Collection date](#)[Collection date \(AD\)](#): December 1st 1909

255 Collector: Mission Gruvel

Museum label: Arca (Senilia) senilis Linné, Baie de Hann, Pointe de Bel Air, plage à basse mer, M Gruvel, 1.XII.1909

MNHN-IM-2022-4606

Donax rugosus

260 Dakar, Bay of Hann (14.71°N, 17.42°W)

Articulated specimen with remains of flesh and hinge ligament.

SacA-68818: 526 ± 18 BP

$F^{14}\text{C} = 0.9366 \pm 0.0022$

$\delta^{13}\text{C} = 0.33 \text{‰ VPDB}$

265 [Collection date](#)[Collection date \(AD\)](#): April 1908

Collector: Mission Gruvel

Museum label: Donax rugosus Linné, Baie de Hann à basse mer, IV 08, Mission Gruvel

MNHN-IM-2022-4598

270 *Bucardium ringens*

Dakar, Bay of Hann at low tide (14.71°N, 17.42°W)

An isolated valve with remains of the hinge ligament.

SacA-68810: 628 ± 17 BP

$F^{14}\text{C} = 0.9247 \pm 0.0019$

275 $\delta^{13}\text{C} = 0.68 \text{‰ VPDB}$

[Collection date](#)[Collection date \(AD\)](#): April 1908

Collector: Mission Gruvel

Museum label: Cardium ringens Gmelin, Baie de Hann à basse mer, IV.08, Mission Gruvel

280 MNHN-IM-2022-4616

Ostrea stentina

Dakar, beach of Hann, posts of the pontoon (14.71°N, 17.42°W)

An isolated valve with remains of flesh

SacA-68835: 539 ± 19 BP

285 $F^{14}\text{C} = 0.9351 \pm 0.0022$

$\delta^{13}\text{C} = 1.56 \text{‰ VPDB}$

~~Collection date~~Collection date (AD): 1947

Collector: Roger Sourie

Museum label: Ostrea stentina Payr Dakar (plage de Hann, piles du ponton) M Sourie 1947

290 3.1.4 Samples from Republic of Guinea

MNHN-IM-2022-4601

Bucardium ringens

Los Islands, Roume Island at low tide (9.46°N, 13.79°W)

A fresh-looking isolated valve.

295 SacA-68813: 857 ± 39 BP

$F^{14}C = 0.8988 \pm 0.0043$

$\delta^{13}C = -0.40$ ‰ VPDB

~~Collection date~~Collection date (AD): December 20th 1909

Collector: Mission Gruvel

300 Museum label: Cardium ringens Gmelin; Ile Roumé, archipel de Los, à basse mer, 20.XII.09, Mission Gruvel

MNHN-IM-2022-4618

Pseudochama gryphina

Los Islands, Tamara Island (9.46°N, 13.83°W)

305 An articulated specimen.

SacA-68820: 502 ± 19 BP

$F^{14}C = 0.9395 \pm 0.0022$

$\delta^{13}C = 1.52$ ‰ VPDB

~~Collection date~~Collection date (AD): 1909-1910

310 Collector: Mission Gruvel

Museum label: Chama gryphina Lm, Tamara, Guinée, mission Gruvel, 1909-1910

Note: It is possible that this sample was also collected in December 1909 as sample MNHN-IM-2022-4601

3.1.5 Sample from Sierra Leone

MNHN-IM-2022-4611

315 *Ostrea stentina*

Near Cape Saint Ann (7.56°N, 12.94°W)

Articulated specimen with remains of flesh.

SacA-68830: 464 ± 18 BP

$F^{14}C = 0.9439 \pm 0.0021$

320 $\delta^{13}C = 1.04 \text{ ‰ VPDB}$

~~Collection date~~ [Collection date \(AD\)](#): 1912

Collector: Mission Gruvel

Museum label: Sierra Léone près Cap Ste Anne, m. Gruvel, 1912

3.1.6 Samples from Benin

325 MNHN-IM-2022-4591

Senilia senilis

Ahémé Lake (6.42°N, 1.96°E)

Articulated specimen with well-preserved periostracum

SacA-68823: 414 ± 18 BP

330 $F^{14}C = 0.9498 \pm 0.0021$

$\delta^{13}C = -4.76 \text{ ‰ VPDB}$

~~Collection date~~ [Collection date \(AD\)](#): February 1910

Collector: Mission Gruvel

Museum label: Arca (*Senilia*) *senilis* Linné, Lac Ahémé Dahomey, Mission Gruvel, II.1910

335 [Note: Ahémé Lake is located 10 km from the coast, exhibiting only limited connection with the coastal lagoons. Thus, we doubt that this sample is representative of the Atlantic Ocean, and hence we discarded it in our calculation of regional R and \$\Delta R\$ for West Africa.](#)

MNHN-IM-2022-4600

340 *Bucardium ringens*

Cotonou, dredging at a water depth of 20-25 meters (6.33°N, 2.39°E)

A fresh isolated valve of a juvenile.

SacA-68812: 606 ± 18 BP

$F^{14}C = 0.9273 \pm 0.0020$

345 $\delta^{13}C = 0.26 \text{ ‰ VPDB}$

~~Collection date~~ [Collection date \(AD\)](#): February 1910

Collector: Mission Gruvel

Museum label: *Cardium ringens*, Cotonou, mer, II.1910, sac 372, Mission Gruvel

Note: The information that the sample came from a dredging at 20-25 meters water depth in front of Cotonou can be found in

350 Dautzenberg (1912).

MNHN-IM-2022-4602

Bucardium ringens

La Bouche du Roi, Grand Popo, beach (6.29°N, 1.92°E)

355 An isolated valve with remains of the hinge ligament.

SacA-68814: 527 ± 17 BP

F¹⁴C = 0.9365 ± 0.0020

δ¹³C = 0.25 ‰ VPDB

~~Collection date~~ [Collection date \(AD\)](#): February 1910

360 Collector: Mission Gruvel

Museum label: Cardium ringens Gmelin, Bouche du Roi, Gd Popo, plage, II.1910, Mission Gruvel.

Note: Three labels mention the same location, but one label mentions the Catumbella estuary (Angola, June 17th 1910). We believe the sample is from Grand Popo.

3.1.7 Samples from Ivory Coast

365 MNHN-IM-2022-4595

Bucardium ringens

Grand Bassam, beach (5.19°N, 3.73°W)

An isolated valve with remains of the hinge ligament.

SacA-68807: 507 ± 18 BP

370 F¹⁴C = 0.9388 ± 0.0021

δ¹³C = 0.29 ‰ VPDB

~~Collection date~~ [Collection date \(AD\)](#): 1909-1910

Collector: Mission Gruvel

Museum label: Cardium ringens Gmelin, plage de Gd Bassam 1909-10, mission Gruvel.

375

MNHN-IM-2022-4597

Bucardium ringens

Jacqueville, beach (5.19°N, 4.42°W)

An isolated valve of a juvenile with remains of the hinge ligament.

380 SacA-68809: 995 ± 18 BP

F¹⁴C = 0.8835 ± 0.0020

δ¹³C = 0.03 ‰ VPDB

~~Collection date~~ [Collection date \(AD\)](#): January 10th 1910

Collector: Mission Gruvel

385 Museum label: *Cardium ringens* Gmel., Jacqueville Côte d'Ivoire, plage, 19.I.10, Mission Gruvel.

3.1.8 Sample from Gabon

MNHN-IM-2022-4613

Ostrea stentina

Port-Gentil (0.71°S, 8.79°E)

390 An isolated valve with remains of flesh.

SacA-68832: 497 ± 19 BP

$F^{14}C = 0.9401 \pm 0.0022$

$\delta^{13}C = 2.24 \text{ ‰ VPDB}$

~~Collection date~~Collection date (AD): 1948

395 Collector: Charles Roux' mission

Museum label: Port Gentil, M Roux, 1949.

Note: Charles Roux writes in 1949 (Roux, 1949) that he was in the Port-Gentil area during the year 1948. We can understand that he was already back to France in 1949. Hence, the ~~collection date~~Collection date must be 1948 AD.

3.1.9 Samples from Republic of Congo

400 MNHN-IM-2022-4614

Ostrea stentina

Loango (4.66°S, 11.80°E)

An isolated valve with remains of flesh.

SacA-68833: 571 ± 19 BP

405 $F^{14}C = 0.9314 \pm 0.0022$

$\delta^{13}C = 1.38 \text{ ‰ VPDB}$

~~Collection date~~Collection date (AD): 1890

Collector: Augusto Nobre

Museum label: *Ostrea stentina* Payr Loango M. Nobre 1890

410

MNHN-IM-2022-4604

Donax rugosus

Pointe-Noire (4.76°S, 11.84°E)

A fresh isolated valve from a juvenile specimen.

415 SacA-68816: 447 ± 18 BP

$F^{14}C = 0.9459 \pm 0.0021$

$\delta^{13}\text{C} = 0.84 \text{ ‰ VPDB}$

~~Collection date~~[Collection date \(AD\)](#): December 1936 – April 1937

Collector: Edgard Aubert de la Rüe

420 Museum label: Pte Noire, Aubert de la Rüe, 1937

Note: Edgard Aubert de la Rüe was in Congo from 18/12/1936 to 16/04/1937 as evidences by his field books kept in the archives of the Musée du Quai Branly (files 2AP/62 to 2AP/64)

3.1.10 Samples from Angola

MNHN-IM-2022-4590

425 *Senilia senilis*

Cabinda (5.55°S, 12.20°E)

Articulated specimen with well-preserved periostracum.

SacA-68822: 584 ± 17 BP

$F^{14}\text{C} = 0.9298 \pm 0.0020$

430 $\delta^{13}\text{C} = -1.15 \text{ ‰ VPDB}$

~~Collection date~~[Collection date \(AD\)](#): 1885-1887

Collector: Paul Hesse

Museum label: Cabinda, Cabinda, Angola; C.R. Boettger coll. 1909

Note: The shell was donated by Caesar R. Boettger to the MNHN in 1909 (Oliver and von Cosel, 1992) but collected earlier
435 by Paul Hesse when Hesse was leaving in Banana (Democratic Republic of Congo) south of Cabinda (Boettger, 1912).
Boettger (1912, p. 110) writes that Hesse's collection includes a number of *Senilia senilis* specimens from Cabinda. The collection date is unfortunately not provided. However, Hesse was employed by a trading company in Banana by the end/beginning 1884/1885 since at least after March 1886 (Westhoff, 1886). Mollusc specimens reported in Boettger (1912) were collected by Hesse between 1885 and 1886. Also, Hesse collected reptile specimens in Cabinda in 1885 and 1887
440 (Boettger, 1898). Thus, we believe that the MNHN specimen must have been collected between 1885 and 1887 [AD](#).

MNHN-IM-2022-4594

Senilia senilis

Cabinda (5.55°S, 12.20°E)

445 An isolated valve with well-preserved periostracum.

SacA-68826: 536 ± 19 BP

$F^{14}\text{C} = 0.9355 \pm 0.0022$

$\delta^{13}\text{C} = -3.11 \text{ ‰ VPDB}$

~~Collection date~~[Collection date \(AD\)](#): June 6th 1921

450 Collector: Unknown
Museum label [Staad collection]: Arca senilis Lin, Cabenda, Africa, Guinea, bought just over 1d on June 6th 1921 in Grays Jun rd, (some of the specimens at B. M. are more than double the size of mine).

MNHN-IM-2022-4589

455 *Senilia senilis*

Luanda, beach (8.78°S, 13.27°E)

Articulated specimen with well-preserved periostracum.

SacA-68821: 538 ± 19 BP

F¹⁴C = 0.9353 ± 0.0022

460 δ¹³C = -0.16 ‰ VPDB

~~Collection date~~Collection date (AD): May 18th 1910

Collector: Mission Gruvel

Museum label: Arca (*Senilia*) *senilis* Linné, St Paul de Loanda, plage, Mission Gruvel, 18.V.1910.

465 MNHN-IM-2022-4605

Donax rugosus

Luanda, beach (8.82°S, 13.21°E)

Articulated specimen with remains of flesh and hinge ligament.

SacA-68817: 528 ± 18 BP

470 F¹⁴C = 0.9364 ± 0.0021

δ¹³C = 0.82 ‰ VPDB

~~Collection date~~Collection date (AD): May 18th 1910

Collector: Mission Gruvel

Museum label: *Donax rugosus* Linné, St Paul de Loanda plage, 18.V.10, Mission Gruvel.

475

MNHN-IM-2022-4596

Bucardium ringens

Bay of Lobito, near the peninsula (12.33°S, 13.56°E)

An isolated valve.

480 SacA-68808: 595 ± 17 BP

F¹⁴C = 0.9286 ± 0.0020

δ¹³C = 1.51 ‰ VPDB

~~Collection date~~Collection date (AD): June 1910

Collector: Mission Gruvel

485 Museum label: *Cardium ringens* Gmelin, Baie de Lobito côté presqu'île, VI.1910, mission Gruvel.

MNHN-IM-2022-4617

Ostrea stentina

Moçâmedes (15.18°S, 12.14°E)

490 A fresh isolated valve.

SacA-68836: 568 ± 18 BP

$F^{14}C = 0.9317 \pm 0.0021$

$\delta^{13}C = 1.75$ ‰ VPDB

~~Collection date~~Collection date (AD): 1910

495 Collector: Mission Gruvel

Museum label: Mossamédès, m Gruvel, 1910

3.2 West African marine reservoir ages

The vast majority of the calculated ΔR values, with a weighted mean ~~n~~ average value of ~~-77-72~~ \pm ~~47-42~~ ^{14}C yrs (1sd, n = ~~2524~~), which corresponds to an ~~averaged~~ weighted mean R value of ~~400-406~~ \pm ~~59-56~~ ^{14}C yrs (1sd, n = ~~2524~~), are typical of low latitudes marine reservoir age values (Bard, 1988; Bard et al., 1994) (Table S1 in the Supplement, Fig. 1). Note that all averaged R and ΔR values were calculated according to the methodology recommended in the Marine Reservoir Correction Database (Reimer and Reimer, 2001; <http://calib.org/marine/AverageDeltaR.html>; last seen 31/05/2023). Our results agree perfectly with those already obtained (Ndeye, 2008) from the Nouadhibou-Cansado Bay area (Mauritania; Nh in Fig. 1) and the Dakar area (Senegal; Dk in Fig. 1); the only two areas that we can compare our results to.

505 No significant interspecific differences were observed. This is best illustrated for the localities where reservoir age values were obtained from at least two different species for the same calendar time. In the Dakar area (Senegal; Dk in Fig. 1) for years 1908-1909 AD, we present data for 5 species (*Bucardium ringens*, *Donax rugosus*, *Mactra glabrata*, *Ostrea stentina*, *Senilia senilis*) (Ndeye, 2008; this study) all clustering within a range of [413;546] ([min; max]) with an average ΔR value of ~~-16-18~~ \pm 56 ^{14}C yrs (1sd, n = 6) (corresponding to an average R value of ~~478-465~~ \pm 55 ^{14}C yrs). This was also the case for Luanda (Angola; Lu in Fig. 1) in the ~~year~~ 1910 AD, with two species (*Donax rugosus* and *Senilia senilis*) yielding the same reservoir age values. This was further supported for the area of Nouadhibou-Cansado Bay (Mauritania) showing the same pattern (Ndeye, 2008; this study), although one sample ~~over-out of~~ four was likely an outlier (*Bucardium ringens* with # MNHN-IM-2022-4599). The fact that species living in very different ecological habitats (e.g., *Senilia senilis* in lagoons/semi-enclosed bays and *Donax rugosus* on beaches exposed to heavy surf; see also section material) show similar reservoir age values (R or ΔR) suggests that the habitat only exerts a minor influence on measured reservoir age in this region. The fact that all

investigated species in this study correspond to suspension feeders further implies that suspension feeders are suitable material for reservoir age reconstruction.

Unlike semi-isolated basins such as the [Baltic Sea \(Lougheed et al., 2013\)](#) and Black Sea (Soulet et al., 2019), where the radiocarbon system is closely linked to the local [oxygen/carbon stable isotopic system respectively](#), the open-ocean coastal region of West Africa is characterized by the lack of any relationship between reservoir age values (R or ΔR) and stable oxygen and carbon isotope compositions (r^2 of 0.02 and 0.001, respectively), as inferred from our results.

3.3 Marine reservoir evolution over time

The local marine reservoir age were averaged over 5-yr windows ([1886-1890 [AD](#)]-[1891-1895 [AD](#)] and so on), excluding the five outliers discussed in section 3.5. Sample with radiocarbon lab # AA-70015 (see Table S1 in the Supplement) is a single value from 1916 [AD](#) and was averaged with samples from years 1912 [AD](#). We also calculated global marine reservoir age as the difference between the Marine20 and IntCal20 calibration curves. The evolution of the marine reservoir age of coastal West Africa (pink symbols in Fig. 2) shows a similar trend as that of the global marine reservoir age (black line in Fig. 2) with values declining steadily with time since ca. 1900 AD.

The ^{14}C age evolution of the global ocean (Marine20 calibration curve; Heaton et al., 2020) is constructed using the global carbon cycle model BICYCLE (Köhler et al., 2006; Köhler and Fischer, 2006, 2004; Köhler et al., 2005). This box model incorporates a globally averaged atmospheric box and modules of the terrestrial (7 boxes) and oceanic (10 boxes) components of the carbon cycle. It is driven by temporal changes in the boundary conditions mimicking changing climate and simulates changes in the carbon cycle including ^{14}C . To construct the Marine20 calibration curve, the BICYCLE model was revised to allow the atmospheric CO_2 and F^{14}C to be specified externally (Heaton et al., 2020). [While the modelled Marine20 \(global surface ocean\) radiocarbon age suggest constant values between 1900 and 1950 AD, our measured marine reservoir age R indicates instead a decreasing trend during that period, as a consequence of increasing atmospheric Intcal20 radiocarbon age. This observation of decreasing trend for R in West Africa between 1900 and 1950 AD could possibly reflect atmospheric \$^{14}\text{CO}_2\$ ageing following enhanced fossil fuel emissions to the atmosphere by burning \(e.g., Suess, 1955; Tans et al., 1979\). The global marine reservoir age evolution calculated as the difference between Marine20 and Intcal20 calibration curves \(Fig.1\) is thus also an output of the revised BICYCLE model. The fact that the trend in our measured marine reservoir age is similar to that of the globally modelled ones strongly suggest that global carbon cycle and climate are the first order drivers of the coastal West African marine reservoir age rather than local effects.](#)

3.4 Marine reservoir age off equatorial Ogooué and Congo rivers

Large rivers draining equatorial Africa as the Ogooué and Congo rivers inject massive amounts of freshwater into the Atlantic Ocean (Lambert et al., 2015; Milliman and Farnsworth, 2011) leading to extensive sea surface salinity negative anomalies (Martins and Stammer, 2022). The sea surface salinity negative anomalies are associated with net primary productivity positive anomalies that are likely caused by the nutrient-rich river plumes from the Ogooué and Congo Rivers (Martins and Stammer,

2022). From a radiocarbon perspective, such net primary productivity positive anomalies should imply an increased uptake of atmospheric CO₂ through intensified biological pump. As a result, the reservoir age should be lower than average. The Congo River represents the second largest supplier of dissolved organic carbon (DOC) to [the global ocean](#) with ~5% of the land to ocean DOC flux (Spencer et al., 2016; Coynel et al., 2005; Richey et al., 2022). The DOC exported by the Congo river is ¹⁴C-modern (Marwick et al., 2015; Spencer et al., 2012) and experiments showed that 45% of the Congo River DOC can be photo-mineralized by sunlight (Spencer et al., 2009; Richey et al., 2022). Dissolved inorganic carbon (DIC) released from the photo-mineralisation of the Congo River DOC should also be ¹⁴C-modern. Thus, this modern DOC-derived DIC should impact the marine reservoir age towards values lower compared to average. There is a lack of available data to estimate the age and flux of dissolved CO₂ discharged by the Congo river into the ocean (Richey et al., 2022). Nevertheless, the marine reservoir age value measured at Port-Gentil (Gabon) close to the Ogooué river outlet is lower than [the regional weighted mean value](#) ($\Delta R = -106 \pm 63$ ¹⁴C years, corresponding to $R = 329 \pm 21$ ¹⁴C yrs) (PG in Fig. 1). The marine reservoir age measured in Pointe-Noire (Republic of Congo) ~150 km north of the Congo river outlet is also lower than [the regional weighted mean value](#) ($\Delta R = -156 \pm 64$ ¹⁴C yrs; $R = 289 \pm 20$ ¹⁴C yrs) (PN in Fig. 1). These values could be interpreted as having been influenced by the Ogooué and Congo Rivers discharges. However, all other localities close to the Congo River outlet had marine reservoir age close to the [average regional weighted mean value](#) (Lo, Ca and Lu, in Fig. 1). Instead the lower values observed in Port-Gentil (Gabon) and Pointe-Noire (Republic of Congo) are from years 1948 and 1937 suggesting that these lower values are in line with the declining global marine reservoir evolution linked to [the atmospheric CO₂, ¹⁴C ageing linked to ¹⁴C-dead input from fossil fuel burning \(Suess effect\) global climate and carbon cycle changes](#) (see section 3.3). The impact of the African equatorial rivers on the local/regional coastal marine reservoir age, if any, cannot be inferred from our results.

3.5 Outlier specimens

Mean marine reservoir age values (R and ΔR) are provided for West Africa based on our data, excluding 5 samples. These particular samples display much larger values with ΔR values ranging from 209 to 454 ¹⁴C yrs or R values ranging from 701 to 912 ¹⁴C yrs. Three specimens out of the five outlier samples correspond to *Bucardium ringens* specimens. We analysed 8 *Bucardium ringens* specimens. These 3 outlier specimens display reservoir age (R and ΔR) values that clearly disagree with neighbouring data (Nouadhibou-Cansado Bay, Loos Islands and Ivory Coast areas; Nh, LI and IC in Fig. 1). The Museum number of these specimens are MNHN-IM-2022-4597, MNHN-IM-2022-4599 and MNHN-IM-2022-4601. We do not expect that these larger values compared to those for neighbouring individuals come from the species feeding practice as they are all suspension feeders like all other investigated specimens. Similarly, we showed that the difference in the habitat [in this region](#) does not impact the [species](#) reservoir ages. Instead *Bucardium ringens* lives in the open coast from 5-10 meters to about 50 meters depth. Shells are commonly cast ashore on beaches but live-taken specimens are rare (von Cosel and Gofas, 2019). [Two](#) of [these the samples that are outliers](#) [were](#) collected at low tide (Roume Island in the Loos Islands; Republic of Guinea) [or on a beach \(Jacqueville; Ivory Coast\)](#) [and was devoid of any remain of flesh or hinge ligament](#). It is thus possible that [these this](#) outlier samples [were](#) a transported subfossil samples that died a century or more before collection date. [The](#)

two other outlier samples had small remain of the hinge ligament (Nouadhibou; Mauritania and Jacqueville; Ivory Coast). It may be possible that these samples are also subfossil specimens. In this case, the hinge ligament must have been partially preserved owing to very favourable environmental conditions (Forman et al., 2004; Huntley et al., 2021). Alternatively, these outliers are not subfossil specimens and unlike the other studied species here, the habitat may exert an influence on R and ΔR values measured in *B. ringens*. Nevertheless, Finally, we cannot fully rule out that these higher values represent some sub-annual variability of up to 200 ^{14}C in the local marine reservoir age as evidenced elsewhere (Jones et al., 2007, 2010). Although, five *Bucardium ringens* samples out of eight displayed reservoir age values in agreement with the neighbouring reservoir age values, this specie might not be the best suited for reservoir age reconstruction or for sediment/archaeological dating.

The two remaining outliers are *Ostrea stentina* specimens from the El Jadida area (Morocco; eJ in Fig. 1). The sample from El Jadida beach was a single valve looking fresh and collected from the beach (museum # MNHN-IM-2022-4609). Based on the older ^{14}C age of this specimen, we cannot rule out that this sample could actually be a subfossil specimen. The specimen with museum # MNHN-IM-2022-4608 collected in the Sidi Moussa lagoon (south of El Jadida) was a specimen with the articulated valves and remains of flesh was still inside the shell, meaning the specimen was still alive when collected. Variations in the reservoir age could be explained by coastal upwelling that impacts some regions of the Atlantic coast of Morocco and Western Sahara (Freudenthal et al., 2001; Barton et al., 1998). Upwelled waters are depleted in ^{14}C relative to the sea surface potentially causing larger reservoir age values (R or ΔR) like off Portugal (Monge Soares, 1993; Monge Soares and Alveirinho Dias, 2006), California (Kennett et al., 1997), Peru (Kennett et al., 2002; Fontugne et al., 2004; Jones et al., 2007, 2010) or Southern Arabian coast (Southon et al., 2002). Conversely, upwelled waters can also be nutrient-rich causing intensified ocean CO_2 uptake through enhanced primary production and biological pump (Williams and Follows, 2011), in that case, one could expect low-latitude average or decreased reservoir age values (R or ΔR). Off Morocco and Western Sahara, the second hypothesis appears most likely as coastal upwelling in this area is known to bring nutrient-rich waters to the surface ocean (Barton et al., 1998; Freudenthal et al., 2001), although to our knowledge no direct measurement of the ^{14}C content of coastal waters in this region has been published yet. However, according to recent studies the El Jadida area is only weakly impacted by upwelling (Lourenço et al., 2020; Cropper et al., 2014), suggesting average reservoir age values instead of larger ones. Another explanation could be linked to the local hydrology of the Sidi Moussa lagoon. Despite the lagoon is being permanently connected to the ocean, it receives waters from rainfall and resurgences that can have an impact on the salinity in the upstream section of the lagoon (Cheggour et al., 2001). As the surrounding rocks are calcareous sandstones (Manaan, 2003), one could hypothesise that freshwaters feeding the lagoon might be depleted in ^{14}C due to carbonate dissolution in the lagoon watershed causing a hardwater effect and thus a larger reservoir age. A last explanation could be due to an imperfect cleaning of the shell. For *Ostrea stentina*, sediment can be trapped between the growing layers of the shell. If this sediment contains old detrital carbonates and was not perfectly removed before ^{14}C measurement, the ^{14}C age of the shell will appear older, and the reservoir age larger. Additional reservoir age reconstructions from this region on different species would be require to validate the larger reservoir age values reconstructed from the El Jadida area.

4 Conclusion

615 The analysis of pre-bomb suspension-feeding bivalves collected along coastal West Africa from 33°N to 15°S provides marine
reservoir ages that are quite homogenous, with a mean ΔR value of $-77-72 \pm 47-42$ ^{14}C yrs (1sd, n = 2524) and a mean R value
of $400-406 \pm 59-56$ ^{14}C yrs (1sd, n = 2524). When including the robust dataset from Ndeye (2008), the resulting mean ΔR and
R values for coastal West Africa are $-62-54 \pm 51$ ^{14}C years (1sd, n = 3332) and $416-411 \pm 61$ ^{14}C years (1sd, n = 3332),
620 ~~climate-atmospheric~~ ^{14}C changes rather than by local effects.

Our results for different species yield similar marine reservoir age values, indicating that the ecological habitat only has a
second-order impact on the reservoir age reconstruction, if any. Nevertheless, we suspect that *Bucardium ringens* might not
be best suited for marine reservoir age reconstruction as corresponding shells are typically not found alive on sample collecting
sites. Additionally, ages obtained on *Ostrea stentina* could be possibly influenced by the presence of sediment within the
625 growing shell layers if not fully removed after the cleaning process.

Despite these new data, large portions of the West African coast still remain to be investigated for reservoir age reconstructions,
in particular off Western Sahara and Canarias Islands, Sierra Leone-Liberia, Nigeria and Namibia.

Author contribution statement

GSoulet designed the study and raised the funding. SG, PM, GSoulet and GSiani selected the specimens in the MNHN
630 collections. GSoulet carried out the sample preparation with assistance of ML and FF. FD performed stable isotopes
measurements. GSoulet performed reservoir calculations and analysed and discussed the data with GB, GSiani and SG.
GSoulet wrote the manuscript with inputs from all co-authors.

Acknowledgements

All authors thank Michel Fontugne, an anonymous reviewer and Paula Reimer for reviewing the manuscript. We are grateful
635 to the Muséum National d'Histoire Naturelle (Paris, France) for providing the samples. We thank the LMC14 staff (Laboratoire
de Mesure du Carbone-14) and the CNRS-INSU ARTEMIS national radiocarbon AMS facility for providing radiocarbon
measurements published in this study. The study was funded by the French national program INSU-LEFE (ResWA project –
Pre-bomb Reservoir ages for the Western coast of Africa). I (GS) thank Ifremer in Brest and Sète for supporting my research.
Finally, this study was carried out and the paper written during my part-time parental leave. I dedicate this article to Marian,
640 with whom I have had a wonderful time during this year, growing up together, him as a toddler and me as a father.

Competing interests

The authors declare that they have no conflict of interest.

Data availability

All data present in the paper are available in the text section 3.1 and in Table S1 in the Supplement.

645 References

- Alves, E. Q., Macario, K., Ascough, P., and Bronk Ramsey, C.: The worldwide marine radiocarbon reservoir effect: Definitions, mechanisms, and prospects, *Rev. Geophys.*, 56, 278–305, <https://doi.org/10.1002/2017RG000588>, 2018.
- Alves, E. Q., Macario, K. D., Urrutia, F. P., Cardoso, R. P., and Bronk Ramsey, C.: Accounting for the marine reservoir effect in radiocarbon calibration, *Quat. Sci. Rev.*, 209, 129–138, <https://doi.org/10.1016/j.quascirev.2019.02.013>, 2019.
- 650 [Arnold, J. R. and Anderson, E. C.: The distribution of Carbon-14 in nature. *Tellus*, 9, 28–32, <https://doi.org/10.1111/j.2153-3490.1957.tb01850.x>, 1957.](https://doi.org/10.1111/j.2153-3490.1957.tb01850.x)
- Ascough, P., Cook, G., and Dugmore, A.: Methodological approaches to determining the marine radiocarbon reservoir effect, *Prog. Phys. Geogr. Earth Environ.*, 29, 532–547, <https://doi.org/10.1191/0309133305pp461ra>, 2005.
- Bard, E.: Correction of accelerator mass spectrometry ^{14}C ages measured in planktonic foraminifera: Paleooceanographic implications, *Paleoceanography*, 3, 635–645, <https://doi.org/10.1029/PA003i006p00635>, 1988.
- 655 Bard, E., Arnold, M., Mangerud, J., Paterne, M., Labeyrie, L., Duprat, J., Mélières, M.-A., Sønstegeard, E., and Duplessy, J.-C.: The North Atlantic atmosphere-sea surface ^{14}C gradient during the Younger Dryas climatic event, *Earth Planet. Sci. Lett.*, 126, 275–287, [https://doi.org/10.1016/0012-821X\(94\)90112-0](https://doi.org/10.1016/0012-821X(94)90112-0), 1994.
- Barton, E. D., Arístegui, J., Tett, P., Cantón, M., García-Braun, J., Hernández-León, S., Nykjaer, L., Almeida, C., Almunia, J.,
- 660 Ballesteros, S., Basterretxea, G., Escánez, J., García-Weill, L., Hernández-Guerra, A., López-Laatzén, F., Molina, R., Montero, M. F., Navarro-Pérez, E., Rodríguez, J. M., van Lenning, K., Vélez, H., and Wild, K.: The transition zone of the Canary Current upwelling region, *Prog. Oceanogr.*, 41, 455–504, [https://doi.org/10.1016/S0079-6611\(98\)00023-8](https://doi.org/10.1016/S0079-6611(98)00023-8), 1998.
- Boettger, C. R.: Zur Molluskenfauna des Kongogebiets, *Ann. la Société R. Zool. Malacol. Belgique*, 47, 89–117, 1912.
- Boettger, O.: Katalog der Reptilien-Sammlung im Museum der Senckenbergischen Naturforschenden Gesellschaft in
- 665 Frankfurt am Main, II Teil (Schlangen), Gebrüder Knauer, Frankfurt am Main, 1898.
- Butzin, M., Köhler, P., and Lohmann, G.: Marine radiocarbon reservoir age simulations for the past 50,000 years, *Geophys. Res. Lett.*, 44, 8473–8480, <https://doi.org/10.1002/2017GL074688>, 2017.
- 670 [Carré, M., Bentaleb, I., Blamart, D., Ogle, N., Cardenas, F., Zevallos, S., Kalin, R. M., Ortlieb, L., and Fontugne, M.: Stable isotopes and sclerochronology of the bivalve *Mesodesma donacium*: Potential application to Peruvian paleoceanographic reconstructions, *Palaeogeogr. Palaeoclimatol. Palaeoecol.*, 228, 4–25, <https://doi.org/10.1016/j.palaeo.2005.03.045>, 2005.](https://doi.org/10.1016/j.palaeo.2005.03.045)

- Catry, T., Figueira, P., Carvalho, L., Monteiro, R., Coelho, P., Lourenço, P. M., Catry, P., Tchantchalam, Q., Catry, I., Botelho, M. J., Pereira, E., Granadeiro, J. P., and Vale, C.: Evidence for contrasting accumulation pattern of cadmium in relation to other elements in *Senilia senilis* and *Tagelus adansonii* from the Bijagós archipelago, Guinea-Bissau, *Environ. Sci. Pollut. Res.*, 24, 24896–24906, <https://doi.org/10.1007/s11356-017-9902-8>, 2017.
- 675 Cheggour, M., Chafik, A., Langston, W. ., Burt, G. ., Benbrahim, S., and Texier, H.: Metals in sediments and the edible cockle *Cerastoderma edule* from two Moroccan Atlantic lagoons: Moulay Bou Selham and Sidi Moussa, *Environ. Pollut.*, 115, 149–160, [https://doi.org/10.1016/S0269-7491\(01\)00117-8](https://doi.org/10.1016/S0269-7491(01)00117-8), 2001.
- von Cosel, R. and Gofas, S.: *Marine Bivalves of Tropical West Africa: From Rio de Oro to Southern Angola*, edited by: MNHN and IRD, *Faune et Flore tropicales*, 48, Paris, Marseille, 1104 pp., 2019.
- 680 Cottereau, E., Arnold, M., Moreau, C., Baqué, D., Bavay, D., Caffy, I., Comby, C., Dumoulin, J.-P., Hain, S., Perron, M., Salomon, J., and Setti, V.: Artemis, the new ^{14}C AMS at LMC14 in Saclay, France, *Radiocarbon*, 49, 291–299, <https://doi.org/10.1017/S0033822200042211>, 2007.
- Coynel, A., Seyler, P., Etcheber, H., Meybeck, M., and Orange, D.: Spatial and seasonal dynamics of total suspended sediment and organic carbon species in the Congo River, *Global Biogeochem. Cycles*, 19, n/a-n/a, <https://doi.org/10.1029/2004GB002335>, 2005.
- 685 [Craig, H.: The natural distribution of radiocarbon and the exchange time of carbon dioxide between atmosphere and sea, *Tellus*, 9, 1–17, <https://doi.org/10.1111/j.2153-3490.1957.tb01848.x>, 1957.](https://doi.org/10.1111/j.2153-3490.1957.tb01848.x)
- Cropper, T. E., Hanna, E., and Bigg, G. R.: Spatial and temporal seasonal trends in coastal upwelling off Northwest Africa, 1981–2012, *Deep Sea Res. Part I Oceanogr. Res. Pap.*, 86, 94–111, <https://doi.org/10.1016/j.dsr.2014.01.007>, 2014.
- 690 Dautzenberg, P.: Mission Gruvel sur la côte occidentale d'Afrique (1909-1910): Mollusques marins. *Annales de l'Institut Océanographique*, Paris (Nouvelle Série). 5(3): 1-111, pl. 1-3, 1912.
- Dewar, G., Reimer, P. J., Sealy, J., and Woodborne, S.: Late-Holocene marine radiocarbon reservoir correction (ΔR) for the west coast of South Africa, *The Holocene*, 22, 1481–1489, <https://doi.org/10.1177/0959683612449755>, 2012.
- 695 Dumoulin, J.-P., Comby-Zerbino, C., Delqué-Količ, E., Moreau, C., Caffy, I., Hain, S., Perron, M., Thellier, B., Setti, V., Berthier, B., and Beck, L.: Status report on sample preparation protocols developed at the LMC14 laboratory, Saclay, France: From Sample Collection to ^{14}C AMS Measurement, *Radiocarbon*, 59, 713–726, <https://doi.org/10.1017/RDC.2016.116>, 2017.
- [Fontugne, M., Carré, M., Bentaleb, I., Julien, M., and Lavallée, D.: Radiocarbon reservoir age variations in the south Peruvian upwelling during the Holocene, *Radiocarbon*, 46, 531–537, <https://doi.org/10.1017/S003382220003558X>, 2004.](https://doi.org/10.1017/S003382220003558X)
- 700 [Forman, S.: A review of postglacial emergence on Svalbard, Franz Josef Land and Novaya Zemlya, northern Eurasia, *Quat. Sci. Rev.*, 23, 1391–1434, <https://doi.org/10.1016/j.quascirev.2003.12.007>, 2004.](https://doi.org/10.1016/j.quascirev.2003.12.007)
- Freudenthal, T., Neuer, S., Meggers, H., Davenport, R., and Wefer, G.: Influence of lateral particle advection and organic matter degradation on sediment accumulation and stable nitrogen isotope ratios along a productivity gradient in the Canary Islands region, *Mar. Geol.*, 177, 93–109, [https://doi.org/10.1016/S0025-3227\(01\)00126-8](https://doi.org/10.1016/S0025-3227(01)00126-8), 2001.

- 705 Heaton, T. J., Köhler, P., Butzin, M., Bard, E., Reimer, R. W., Austin, W. E. N., Bronk Ramsey, C., Grootes, P. M., Hughen, K. A., Kromer, B., Reimer, P. J., Adkins, J., Burke, A., Cook, M. S., Olsen, J., and Skinner, L. C.: Marine20—The Marine Radiocarbon Age Calibration Curve (0–55,000 cal BP), *Radiocarbon*, 62, 779–820, <https://doi.org/10.1017/RDC.2020.68>, 2020.
- Heaton, T. J., Bard, E., Bronk Ramsey, C., Butzin, M., Köhler, P., Muscheler, R., Reimer, P. J., and Wacker, L.: Radiocarbon: A key tracer for studying Earth’s dynamo, climate system, carbon cycle, and Sun, *Science* (80-.), 374, <https://doi.org/10.1126/science.abd7096>, 2021.
- 710 Heaton, T. J., Bard, E., Bronk Ramsey, C., Butzin, M., Hatté, C., Hughen, K. A., Köhler, P., and Reimer, P. J.: A response to community questions on the Marine20 radiocarbon age calibration curve: Marine reservoir ages and the calibration of ^{14}C samples from the oceans, *Radiocarbon*, 65, 247–273, <https://doi.org/10.1017/RDC.2022.66>, 2023.
- 715 Herrera, N. D., ter Poorten, J. J., Bieler, R., Mikkelsen, P. M., Strong, E. E., Jablonski, D., and Steppan, S. J.: Molecular phylogenetics and historical biogeography amid shifting continents in the cockles and giant clams (Bivalvia: Cardiidae), *Mol. Phylogenet. Evol.*, 93, 94–106, <https://doi.org/10.1016/j.ympev.2015.07.013>, 2015.
- Hogg, A. G., Heaton, T. J., Hua, Q., Palmer, J. G., Turney, C. S., Southon, J., Bayliss, A., Blackwell, P. G., Boswijk, G., Bronk Ramsey, C., Pearson, C., Petchey, F., Reimer, P., Reimer, R., and Wacker, L.: SHCal20 Southern Hemisphere Calibration, 0–720 55,000 Years cal BP, *Radiocarbon*, 62, 759–778, <https://doi.org/10.1017/RDC.2020.59>, 2020.
- [Huntley, J. W., De Baets, K., Scarponi, D., Linehan, L. C., Epa, Y. R., Jacobs, G. S., and Todd, J. A.: Bivalve mollusks as hosts in the fossil record, in: *The Evolution and Fossil Record of Parasitism*, edited by: De Baets, K. and Huntley, J. W., Springer International Publishing, 251–287, \[https://doi.org/10.1007/978-3-030-52233-9_8\]\(https://doi.org/10.1007/978-3-030-52233-9_8\), 2021.](https://doi.org/10.1007/978-3-030-52233-9_8)
- Kennett, D. J., Ingram, B. L., Erlandson, J. M., and Walker, P.: Evidence for Temporal Fluctuations in Marine Radiocarbon Reservoir Ages in the Santa Barbara Channel, Southern California, *J. Archaeol. Sci.*, 24, 1051–1059, <https://doi.org/10.1006/jasc.1996.0184>, 1997.
- 725 [Kennett, D. J., Lynn Ingram, B., Southon, J. R., and Wise, K.: Differences in \$^{14}\text{C}\$ age between stratigraphically associated charcoal and marine shell from the Archaic Period Site of Kilometer 4, Southern Peru: Old wood or old water?, *Radiocarbon*, 44, 53–58, <https://doi.org/10.1017/S0033822200064663>, 2002.](https://doi.org/10.1017/S0033822200064663)
- 730 Köhler, P. and Fischer, H.: Simulating changes in the terrestrial biosphere during the last glacial/interglacial transition, *Glob. Planet. Change*, 43, 33–55, <https://doi.org/10.1016/j.gloplacha.2004.02.005>, 2004.
- Köhler, P. and Fischer, H.: Simulating low frequency changes in atmospheric CO_2 during the last 740 000 years, *Clim. Past*, 2, 57–78, <https://doi.org/10.5194/cp-2-57-2006>, 2006.
- Köhler, P., Fischer, H., Munhoven, G., and Zeebe, R. E.: Quantitative interpretation of atmospheric carbon records over the last glacial termination, *Global Biogeochem. Cycles*, 19, n/a-n/a, <https://doi.org/10.1029/2004GB002345>, 2005.
- 735 Köhler, P., Muscheler, R., and Fischer, H.: A model-based interpretation of low-frequency changes in the carbon cycle during the last 120,000 years and its implications for the reconstruction of atmospheric $\Delta^{14}\text{C}$, *Geochemistry, Geophys. Geosystems*, 7, n/a-n/a, <https://doi.org/10.1029/2005GC001228>, 2006.

- Lambert, T., Darchambeau, F., Bouillon, S., Alhou, B., Mbega, J.-D., Teodoru, C. R., Nyoni, F. C., Massicotte, P., and Borges, A. V.: Landscape control on the spatial and temporal variability of chromophoric dissolved organic matter and dissolved organic carbon in large African Rivers, *Ecosystems*, 18, 1224–1239, <https://doi.org/10.1007/s10021-015-9894-5>, 2015.
- Lindsay, C. M., Lehman, S. J., Marchitto, T. M., Carriquiry, J. D., and Ortiz, J. D.: New constraints on deglacial marine radiocarbon anomalies from a depth transect near Baja California, *Paleoceanography*, 31, 1103–1116, <https://doi.org/10.1002/2015PA002878>, 2016.
- 745 [Lougheed, B. C., Filipsson, H. L., and Snowball, I.: Large spatial variations in coastal ¹⁴C reservoir age – a case study from the Baltic Sea. *Clim. Past*, 9, 1015–1028. <https://doi.org/10.5194/cp-9-1015-2013>, 2013.](#)
- Lourenço, C. R., Nicastro, K. R., McQuaid, C. D., Krug, L. A., and Zardi, G. I.: Strong upwelling conditions drive differences in species abundance and community composition along the Atlantic coasts of Morocco and Western Sahara, *Mar. Biodivers.*, 50, 15, <https://doi.org/10.1007/s12526-019-01032-z>, 2020.
- 750 Manaán, M.: Étude sédimentologique du remplissage de la lagune de Sidi Moussa, Maroc, PhD thesis, Université Chouaib Doukkali, El Jadida, <https://theses.hal.science/tel-00124571>, 2003.
- Martins, M. S. and Stammer, D.: Interannual variability of the Congo River plume-induced sea surface salinity, *Remote Sens.*, 14, 1013, <https://doi.org/10.3390/rs14041013>, 2022.
- Marwick, T. R., Tamooh, F., Teodoru, C. R., Borges, A. V., Darchambeau, F., and Bouillon, S.: The age of river-transported carbon: A global perspective, *Global Biogeochem. Cycles*, 29, 122–137, <https://doi.org/10.1002/2014GB004911>, 2015.
- 755 Milliman, J. D. and Farnsworth, K. L.: River discharge to the coastal ocean, Cambridge University Press, <https://doi.org/10.1017/CBO9780511781247>, 2011.
- Monge Soares, A.: The ¹⁴C content of marine shells: Evidence for variability in coastal upwelling off Portugal during the Holocene, in: *Isotope techniques in the study of past and current environmental changes in the hydrosphere and the atmosphere proceedings*, edited by: IAEA, Vienna, 471–485, 1993.
- 760 Monge Soares, A. M. and Alveirinho Dias, J. M.: Coastal upwelling and radiocarbon-evidence for temporal fluctuations in ocean reservoir effect off Portugal during the Holocene, *Radiocarbon*, 48, 45–60, <https://doi.org/10.1017/S0033822200035384>, 2006.
- Mook, W. G. and van der Plicht, J.: Reporting ¹⁴C activities and concentrations, *Radiocarbon*, 41, 227–239, <https://doi.org/10.1017/S0033822200057106>, 1999.
- 765 [Moreau, C., Caffy, I., Comby, C., Delqué-Količ, E., Dumoulin, J.-P., Hain, S., Quiles, A., Setti, V., Souprayen, C., Thellier, B., and Vincent, J.: Research and development of the Artemis ¹⁴C AMS facility: Status report, *Radiocarbon*, 55, 331–337, <https://doi.org/10.1017/S0033822200057441>, 2013.](#)
- Ndeye, M.: Marine reservoir ages in Northern Senegal and Mauritania coastal waters, *Radiocarbon*, 50, 281–288, <https://doi.org/10.1017/S0033822200033580>, 2008.
- 770 Okera, W.: Observations on some population parameters of exploited stocks of *Senilia senilis* (= *Arca senilis*) in Sierra Leone, *Mar. Biol.*, 38, 217–229, <https://doi.org/10.1007/BF00388935>, 1976.

- Oliver, P. G. and von Cosel, R.: Taxonomy of tropical west African Bivalves. IV. Arcidae., *Bull. Muséum Natl. d'Histoire Nat.*, 14, 293–381, 1992.
- 775 Reimer, P. J. and McCormac, F. G.: Marine radiocarbon reservoir corrections for the Mediterranean and Aegean Seas, *Radiocarbon*, 44, 159–166, <https://doi.org/10.1017/S0033822200064766>, 2002.
- Reimer, P. J. and Reimer, R. W.: A marine reservoir correction database and on-line interface, *Radiocarbon*, 43, 461–463, <https://doi.org/10.1017/S0033822200038339>, 2001.
- Reimer, P. J., Brown, T. A., and Reimer, R. W.: Discussion: Reporting and calibration of post-bomb ^{14}C data, *Radiocarbon*,
780 46, 1299–1304, <https://doi.org/10.1017/S0033822200033154>, 2004.
- Reimer, P. J., Austin, W. E. N., Bard, E., Bayliss, A., Blackwell, P. G., Bronk Ramsey, C., Butzin, M., Cheng, H., Edwards, R. L., Friedrich, M., Grootes, P. M., Guilderson, T. P., Hajdas, I., Heaton, T. J., Hogg, A. G., Hughen, K. A., Kromer, B., Manning, S. W., Muscheler, R., Palmer, J. G., Pearson, C., van der Plicht, J., Reimer, R. W., Richards, D. A., Scott, E. M., Southon, J. R., Turney, C. S. M., Wacker, L., Adolphi, F., Büntgen, U., Capano, M., Fahrni, S. M., Fogtmann-Schulz, A.,
785 Friedrich, R., Köhler, P., Kudsk, S., Miyake, F., Olsen, J., Reinig, F., Sakamoto, M., Sookdeo, A., and Talamo, S.: The IntCal20 northern hemisphere radiocarbon age calibration curve (0–55 cal kBP), *Radiocarbon*, 62, 725–757, <https://doi.org/10.1017/RDC.2020.41>, 2020.
- Reimer, R. W. and Reimer, P. J.: An online application for ΔR calculation, *Radiocarbon*, 59, 1623–1627, <https://doi.org/10.1017/RDC.2016.117>, 2017.
- 790 [Revelle, R. and Suess, H. E.: Carbon dioxide exchange between atmosphere and ocean and the question of an increase of atmospheric \$\text{CO}_2\$ during the past decades. *Tellus*, 9, 18–27. <https://doi.org/10.1111/j.2153-3490.1957.tb01849.x>, 1957.](https://doi.org/10.1111/j.2153-3490.1957.tb01849.x)
- Richey, J. E., Spencer, R. G. M., Drake, T. W., and Ward, N. D.: Fluvial carbon dynamics across the land to ocean continuum of great tropical rivers, 391–412, <https://doi.org/10.1002/9781119657002.ch20>, 2022.
- Roux, C.: Compte rendu sommaire d'une mission en Afrique Équatoriale Française, *Bull. du Muséum Natl. d'Histoire Nat.*,
795 21, 500–503, 1949.
- Santos, G. M., Southon, J. R., Griffin, S., Beaupre, S. R., and Druffel, E. R. M.: Ultra small-mass AMS ^{14}C sample preparation and analyses at KCCAMS/UCI Facility, *Nucl. Instruments Methods Phys. Res. Sect. B Beam Interact. with Mater. Atoms*, 259, 293–302, <https://doi.org/10.1016/j.nimb.2007.01.172>, 2007.
- Schefuß, E., Eglinton, T. I., Spencer-Jones, C. L., Rullkötter, J., De Pol-Holz, R., Talbot, H. M., Grootes, P. M., and Schneider,
800 R. R.: Hydrologic control of carbon cycling and aged carbon discharge in the Congo River basin, *Nat. Geosci.*, 9, 687–690, <https://doi.org/10.1038/ngeo2778>, 2016.
- Sessa, J. A., Callapez, P. M., Dinis, P. A., and Hendy, A. J. W.: Paleoenvironmental and paleobiogeographical implications of a middle Pleistocene mollusc assemblage from the marine terraces of Baía Das Pipas, southwest Angola, *J. Paleontol.*, 87, 1016–1040, <https://doi.org/10.1666/12-119>, 2013.
- 805 Siani, G., Paterne, M., Arnold, M., Bard, E., Métivier, B., Tisnerat, N., and Bassinot, F.: Radiocarbon reservoir ages in the Mediterranean Sea and Black Sea, *Radiocarbon*, 42, 271–280, <https://doi.org/10.1017/S0033822200059075>, 2000.

- Siani, G., Paterne, M., Michel, E., Sulpizio, R., Sbrana, A., Arnold, M., and Haddad, G.: Mediterranean Sea surface radiocarbon reservoir age changes since the Last Glacial Maximum, *Science* (80-.), 294, 1917–1920, <https://doi.org/10.1126/science.1063649>, 2001.
- 810 [Siegenthaler, U.: Uptake of excess CO₂ by an outcrop-diffusion model of the ocean, *J. Geophys. Res.*, 88, 3599, <https://doi.org/10.1029/JC088iC06p03599>, 1983.](https://doi.org/10.1029/JC088iC06p03599)
- Skinner, L., McCave, I. N., Carter, L., Fallon, S., Scrivner, A. E., and Primeau, F.: Reduced ventilation and enhanced magnitude of the deep Pacific carbon pool during the last glacial period, *Earth Planet. Sci. Lett.*, 411, 45–52, <https://doi.org/10.1016/j.epsl.2014.11.024>, 2015.
- 815 Skinner, L. C. and Bard, E.: Radiocarbon as a dating tool and tracer in paleoceanography, *Rev. Geophys.*, 60, 1–64, <https://doi.org/10.1029/2020RG000720>, 2022.
- Skinner, L. C., Fallon, S., Waelbroeck, C., Michel, E., and Barker, S.: Ventilation of the deep Southern Ocean and deglacial CO₂ rise, *Science* (80-.), 328, 1147–1151, <https://doi.org/10.1126/science.1183627>, 2010.
- Smith, D. A. S.: Polymorphism and population density in *Donax rugosus* (Lamellibranchiata: Donacidae), *J. Zool.*, 164, 429–
- 820 441, <https://doi.org/10.1111/j.1469-7998.1971.tb01327.x>, 1971.
- Soulet, G.: Methods and codes for reservoir–atmosphere ¹⁴C age offset calculations, *Quat. Geochronol.*, 29, 97–103, <https://doi.org/10.1016/j.quageo.2015.05.023>, 2015.
- Soulet, G., Ménot, G., Garreta, V., Rostek, F., Zaragosi, S., Lericolais, G., and Bard, E.: Black Sea “Lake” reservoir age evolution since the Last Glacial — Hydrologic and climatic implications, *Earth Planet. Sci. Lett.*, 308, 245–258,
- 825 <https://doi.org/10.1016/j.epsl.2011.06.002>, 2011.
- Soulet, G., Skinner, L. C., Beaupré, S. R., and Galy, V.: A note on reporting of reservoir ¹⁴C disequilibria and age offsets, *Radiocarbon*, 58, 205–211, <https://doi.org/10.1017/RDC.2015.22>, 2016.
- Soulet, G., Giosan, L., Flaux, C., and Galy, V.: Using stable carbon isotopes to quantify radiocarbon reservoir age offsets in the coastal black sea, *Radiocarbon*, 61, <https://doi.org/10.1017/RDC.2018.61>, 2019.
- 830 Southon, J., Kashgarian, M., Fontugne, M., Metivier, B., and Yim, W. W. S.: Marine reservoir corrections for the Indian Ocean and Southeast Asia, *Radiocarbon*, 44, 167–180, <https://doi.org/10.1017/S0033822200064778>, 2002.
- Spencer, R. G. M., Stubbins, A., Hernes, P. J., Baker, A., Mopper, K., Aufdenkampe, A. K., Dyda, R. Y., Mwamba, V. L., Mangangu, A. M., Wabakanghanzi, J. N., and Six, J.: Photochemical degradation of dissolved organic matter and dissolved lignin phenols from the Congo River, *J. Geophys. Res.*, 114, G03010, <https://doi.org/10.1029/2009JG000968>, 2009.
- 835 Spencer, R. G. M., Hernes, P. J., Aufdenkampe, A. K., Baker, A., Gulliver, P., Stubbins, A., Aiken, G. R., Dyda, R. Y., Butler, K. D., Mwamba, V. L., Mangangu, A. M., Wabakanghanzi, J. N., and Six, J.: An initial investigation into the organic matter biogeochemistry of the Congo River, *Geochim. Cosmochim. Acta*, 84, 614–627, <https://doi.org/10.1016/j.gca.2012.01.013>, 2012.
- Spencer, R. G. M., Hernes, P. J., Dinga, B., Wabakanghanzi, J. N., Drake, T. W., and Six, J.: Origins, seasonality, and fluxes
- 840 of organic matter in the Congo River, *Global Biogeochem. Cycles*, 30, 1105–1121, <https://doi.org/10.1002/2016GB005427>,

2016.

Stuiver, M. and Braziunas, T. F.: Modeling atmospheric ^{14}C influences and ^{14}C ages of marine samples to 10,000 BC, *Radiocarbon*, 35, 137–189, <https://doi.org/10.1017/S0033822200013874>, 1993.

845 Stuiver, M. and Polach, H. A.: Discussion: Reporting of ^{14}C Data, *Radiocarbon*, 19, 355–363, <https://doi.org/10.1017/S0033822200003672>, 1977.

Stuiver, M., Pearson, G. W., and Braziunas, T.: Radiocarbon age calibration of marine samples back to 9000 cal yr BP, *Radiocarbon*, 28, 980–1021, <https://doi.org/10.1017/S0033822200060264>, 1986.

[Suess, H. E.: Radiocarbon concentration in modern wood, *Science*, 122, 415–417, <https://doi.org/10.1126/science.122.3166.415.b>, 1955.](https://doi.org/10.1126/science.122.3166.415.b)

850 [Tans, P. P., De Jong, A. F. M., and Mook, W. G.: Natural atmospheric \$^{14}\text{C}\$ variation and the Suess effect, *Nature*, 280, 826–828, <https://doi.org/10.1038/280826a0>, 1979.](https://doi.org/10.1038/280826a0)

Tisnérat-Laborde, N., Poupeau, J. J., Tannau, J. F., and Paterne, M.: Development of a semi-automated system for routine preparation of carbonate samples, *Radiocarbon*, 43, 299–304, <https://doi.org/10.1017/S0033822200038145>, 2001.

855 Türkmen, A., Türkmen, M., and Tepe, Y.: Biomonitoring of heavy metals from Iskenderun Bay using two bivalve species *Chama pacifica* Broderip, 1834 and *Ostrea stentina* Payraudeau, 1826, *Turkish J. Fish. Aquat. Sci.*, 5, 107–111, 2005.

Westhoff, F.: Die Fauna der Kongo-Mündung, *Jahresbericht der Zool. Sekt. Westfälischen Prov. Vereins für Wiss. und Kunst für das Etatsjahr 1885-86*, 38–40, 1886.

Williams, R. G. and Follows, M. J.: *Ocean dynamics and the carbon cycle: Principles and mechanisms*, Cambridge., Cambridge, 434 pp., 2011.

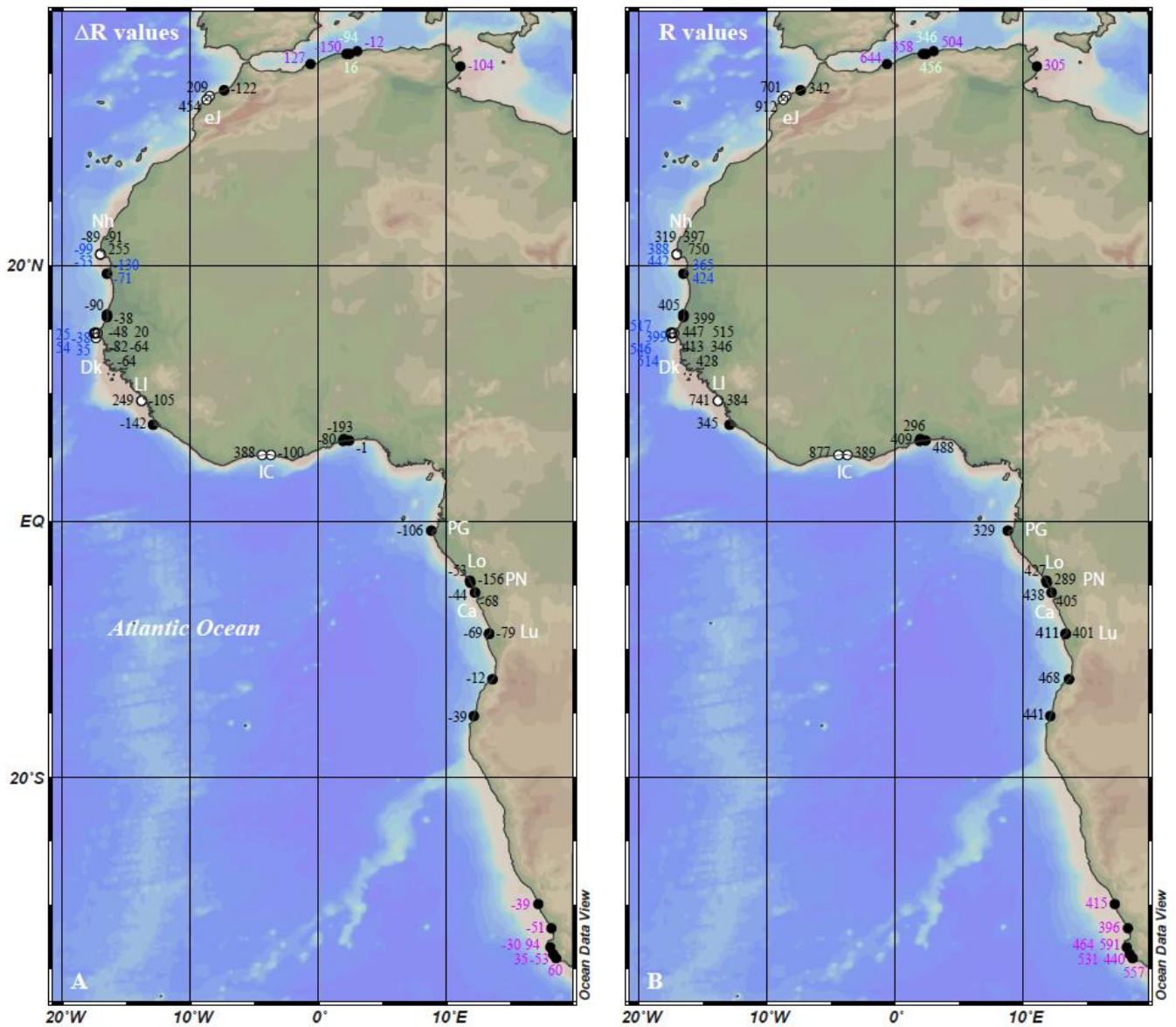
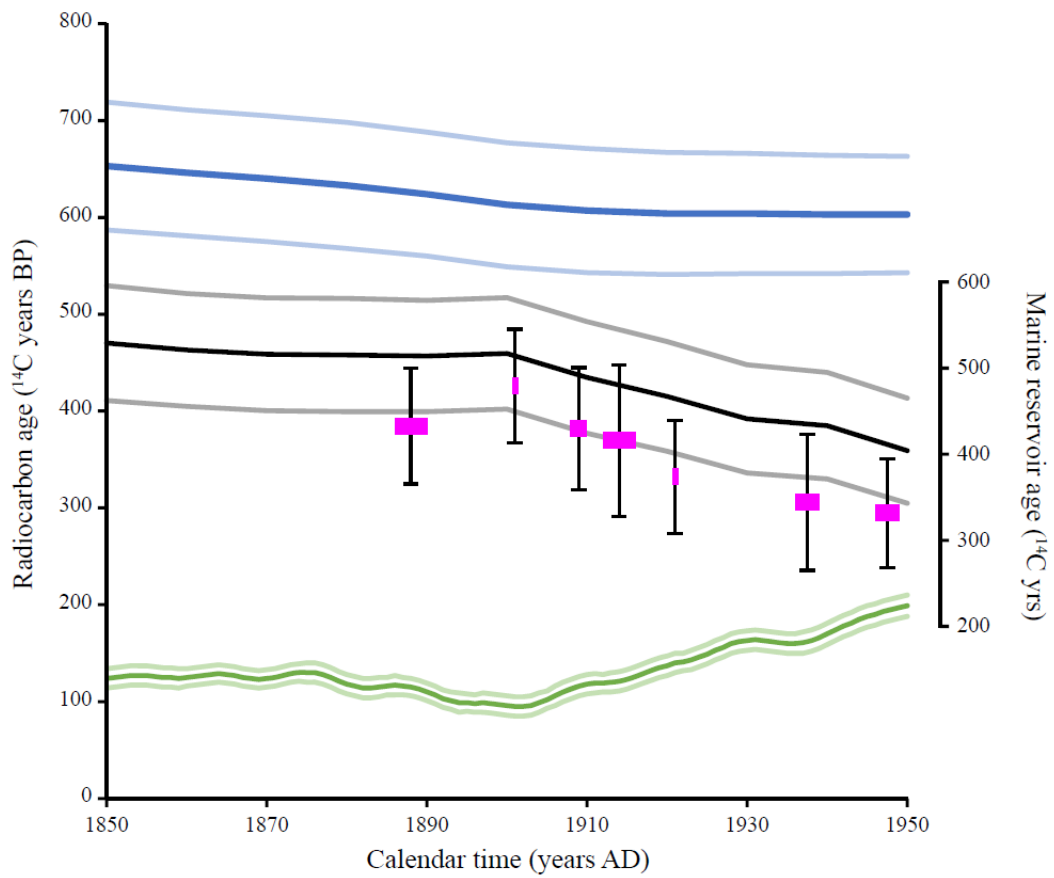


Figure 1: The geographic distribution of marine reservoir age values along the West African coast. A. ΔR values. B. R values. Data shown in black are from this study. Other are selected results from previous studies discussed in the text, converted from their original format (conventional 14C ages and collection dates) to ΔR and R values using the latest calibration curves Marine20 (Heaton et al., 2020) and Intcal20 (Reimer et al., 2020; Hogg et al., 2020), respectively. Data in blue are from Ndeye (2008), data in green are from (Reimer and McCormac, 2002), data in purple are from (Siani et al., 2000) and data in pink are from (Dewar et al., 2012). eJ, Nh, Dk, LI, IC, [PG](#), [Lo](#), [PN](#), [Ca](#) and Lu stand for el Jadida (Morocco), Nouadhibou (Mauritania), Dakar (Senegal), Loos Islands (Republic of Guinea), Ivory Coast, [Port-Gentil \(Gabon\)](#), [Loango \(Republic of Congo\)](#), [Pointe Noire \(Republic of Congo\)](#), [Cabinda \(Angola\)](#) and Luanda (Angola). The map was drawn using Ocean Data View (Schlitzer, Reiner, Ocean Data View, <https://odv.awi.de>, 2022).



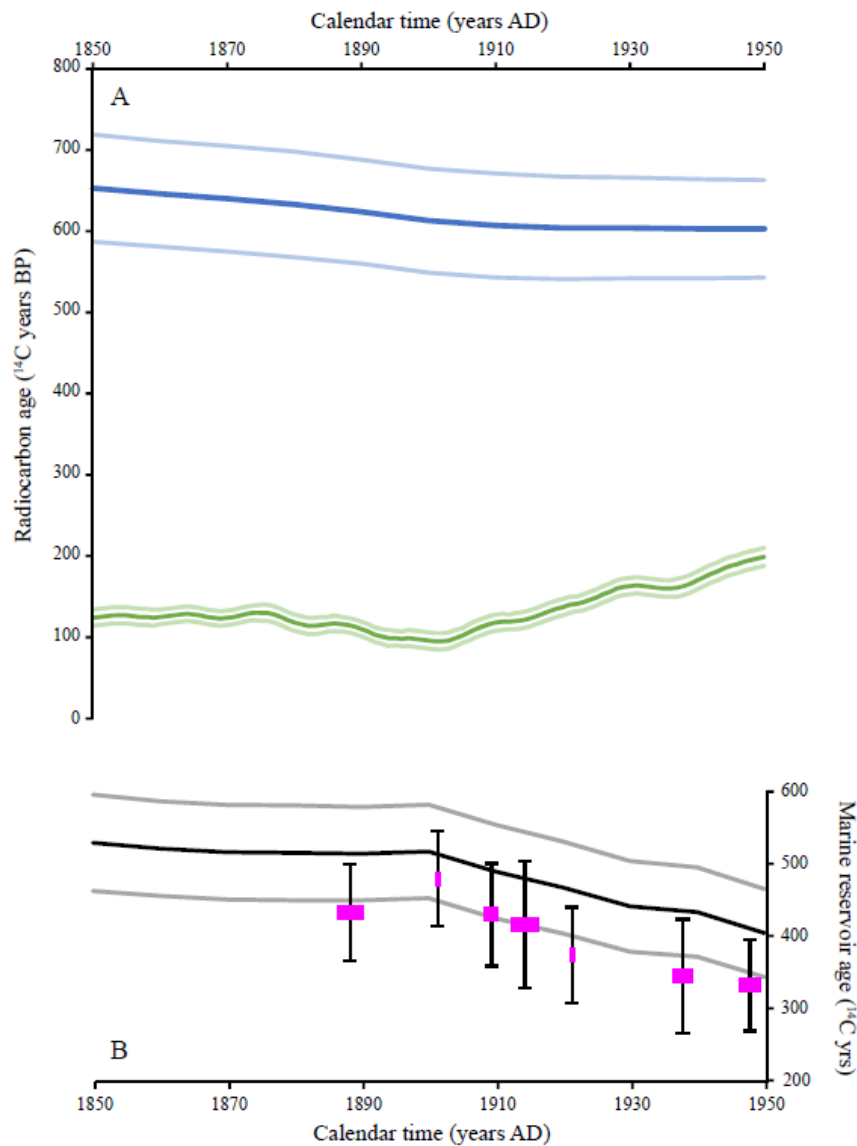


Figure 2: **Left axis A:** The radiocarbon age evolution of the atmosphere (IntCal20; green curve with its light green 1- σ envelope) and of the global ocean (Marine20; blue curve with its light blue 1- σ envelope) between 1850 and 1950 AD. **Right axis B:** The global marine reservoir age (black curve with its grey 1- σ envelope) calculated as the difference between Marine20 and Intcal20 curves. Pink symbols are the coastal West African marine reservoir age calculated averaging data over 5-yr windows. The reported error bars are the maximum of the standard deviation of the averaged data and the individual uncertainty of the averaged data.

875